  Bull. Chem. Soc. Jpn., 60, 2237—2243 (1987)

Hydrogenation of Carbon Monoxide over Solid Catalysts Dispersed in the Liquid Medium. I. Slurry-Phase Fischer-Tropsch Synthesis with Supported Ruthenium Catalysts

Kaoru FUJIMOTO* and Masahiko KAJIOKA
Department of Synthetic Chemistry, Faculty of Engineering, The University of Tokyo, Hongo, Bunkyo-ku, Tokyo 113
(Received October 31, 1986)

Fischer-Tropsch synthesis on supported ruthenium catalysts were operated successfully in the slurry phase, using ethyl cyclohexane solvent, in spite of the high selectivity of waxy products. Titania, fumed silica, and Nb_2O_5 were found to be excellent carriers for ruthenium. A Ru/SiO_2 catalyst yielded a hydrocarbon product with the rate as high as 600 mg(g-cat)$^{-1}$h^{-1} at 240 °C and 40 bar. The optimum metal loading was 2% by weight. Calcination of the catalyst precursor at 300 °C or above caused a marked decrease in the metal dispersion, which was essential for the high catalytic activity and chain-growth ability. The maximum chain-growth probability obtained on a calcined Ru/Al_2O_3 catalyst was 0.94.

Fischer-Tropsch synthesis (F-T synthesis), which produces hydrocarbon mixtures from synthesis gas, is one of the most promising coal liquefaction processes. Usually, the reaction is an exothermic reaction, which generates the heat from 54 to 39 kcal (1 cal_{th}=4.184 J) per mole of CO depending on the product. Therefore, it is quite important, in order to conduct the reaction on a large scale, to remove the heat of reaction effectively from the catalyst bed and to maintain its temperature at the suitable level. Typical reactor systems of the F-T synthesis are a multi-tube fixed bed reactor, a fluidized bed reactor, an ebulating bed reactor, and a slurry bed reactor. The multi-tube fixed bed reactor and the fluidized bed reactor are now in commercial operations.

The slurry bed reactor system was postulated and developed by Koelbel et al. since 1935.[1,2] The process utilizes fine powdery catalysts dispersed in a mineral oil medium, whereinto synthesis gas is fed in the bubble form to carry out the reaction. The characteristic features of the slurry bed reactor are: (1) The reactor structure is quite simple; (2) the removal of reaction heat can be effectively carried out to attain quite a flat temperature profile in the reactor;[2] and (3) it has no wax trouble because the high-boiling product on the catalyst surface is quickly removed by being dissolved into the liquid medium. Thus, the slurry-phase system is thought to be the most economical F-T synthesis reactor system.[3]

Almost all of the works on the slurry-phase F-T synthesis have been carried out by using precipitated iron catalyst or fused iron catalyst. In the present work the activities and selectivities of supported ruthenium catalysts were studied in the slurry-phase in comparing with the gas-phase reaction.

Experimental

Catalyst Preparation and Characterization. Several kinds of alumina were used as carrier materials in this study. γ-Al_2O_3-A (220 m^2g^{-1}) was prepared by hydrolyzing aluminium isopropoxide and calcining in air at 600 °C for 3 h. γ-Al_2O_3-B was a commercially available one (Tokai Konetsu, TKS-99651, 300 m^2mg^{-1}, and γ-Al_2O_3-C (Aerosil Al_2O_3-C, 100 m^2g^{-1}) was obtained from Japan Aerosil Co. γ-Al_2O_3-D was also a commercially available one (Sunbead AN, 340 m^2g^{-1}), γ-Al_2O_3-E (JRC-ALO-3, 123 m^2g^{-1}) and γ-Al_2O_3-F (JRC-ALO-4, 177 m^2g^{-1}) were obtained from Japan Catalyst Society. α-Al_2O_3 was a commercially available one (Tokai Konetsu, TAS-90337, <1 m^2g^{-1}). Other carrier materials than alumina were Aerosil SiO_2, Davison ID SiO_2, TiO_2, Nb_2O_5, ZrO_2, and Th_2O_5. These materials were commercially available ones and were already used by the present authors as carrier materials of ruthenium for the vapor-phase F-T synthesis.[5] Supported ruthenium catalysts were prepared by impregnating carrier materials with $RuCl_3 \cdot 3H_2O$ from its aqueous solution, drying up at 100 °C and then drying overnight at 120 °C in an air oven. The catalyst precursors thus obtained were ground to fine powders (under 150 mesh), calcined if needed, and then activated by reducing in flowing hydrogen at 150 °C for 1 h and 400 or 450 °C for 2 h in series. After the activation, the catalyst was directly introduced in the solvent which had been deoxygenated by bubbling CO_2 for 30 min, and then introduced into the F-T synthesis reactor as a slurry.

The dispersion of ruthenium metal was determined by means of CO chemisorption. Chemisorption was measured at room temperature by using a flow-through cell connected to a glass vacuum system. Catalyst samples were first activated in flowing hydrogen in situ, at 150 °C for 1 h and at 450 °C for 2 h, and then evacuated at 450 °C for 2 h. Chemisorption of CO was determined as the difference between the first isotherm and the second isotherm which was measured following the evacuation for 30 min at room temperature after the measurement of the first isotherm. The metal dispersion was calculated assuming one CO molecule was chemisorbed by one surface ruthenium atom.

Apparatuses and Procedures of Synthesis Gas Reaction and Analysis. The flow sheet of the reaction system is shown in Fig. 1. Synthesis gas reactions were conducted in a stainless steel autoclave reactor (volume 100 cm^3). Only gaseous substances were treated in a flow system, and the gas flow from the reactor was kept at 50 cm^3min^{-1} under the standard temperature and pressure. The effluent from the reactor was withdrawn in the gaseous state through a heated pressure regulator and analyzed by gas chromatographs. Most of the solvent and produced hydrocarbons were refluxed while small parts of product hydrocarbon and solvent came out of the reactor with the unreacted synthesis gas.

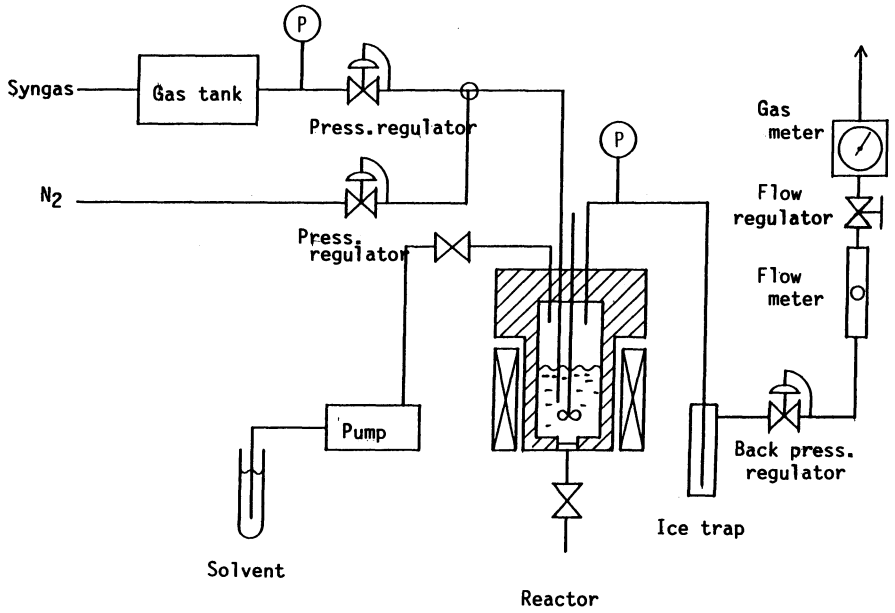

Fig. 1. Reaction apparatus for slurry-phase Fischer-Tropsch synthesis.

The volume of solvent (ethylcyclohexane) was 30 cm^3 and from 2 to 3 gram of catalyst was used for the reaction depending on its catalytic activity. The reaction pressure indicates the total pressure at the reaction temperature, including the vapor pressure of the solvent (about 10 bar). Synthesis gas was introduced from a cylinder through an activated carbon column. Activities and selectivities of the supported ruthenium catalysts were measured mainly under the following conditions: 240 °C, 40 bar, $H_2/CO=2$, and 4 h of reaction, and then the average formation rate of hydrocarbons and the hydrocarbon distribution were calculated.

Gaseous compounds were analyzed on line by gas chromatographs. CO, CH_4, and CO_2 were analyzed by an activated charcoal column using a TCD detector. Light hydrocarbons (C_1—C_6) were analyzed by a Porapak Q column using a FID detector. Liquid products dissolved in the solvent were analyzed after the reaction was over. Hydrocarbons with 2 to 21 carbon atoms were analyzed with a Silicone SE-30 column and hydrocarbons with 11 to 45 carbon atoms were analyzed with a Dexsil 300 GC column, respectively. Eicosane (n-$C_{20}H_{42}$) was used as an internal stan-dard material and a FID detector was used in each analysis

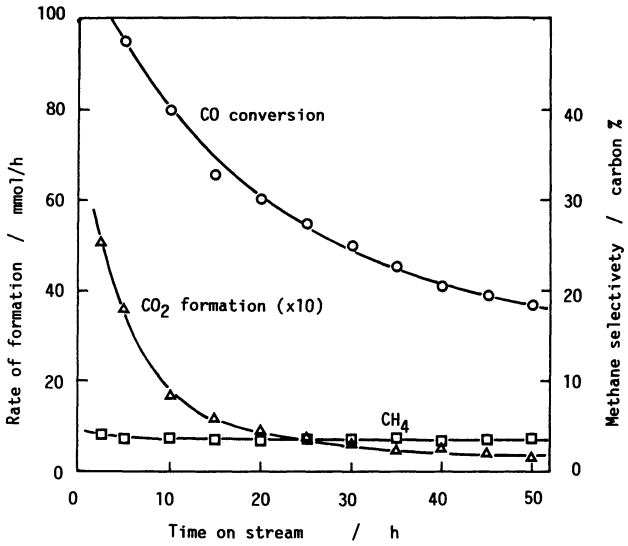

Fig. 2. Changes in the catalytic performance of a Ru/Al_2O_3 catalyst. 2 wt% Ru/γ-Al_2O_3-E, 400 °C calcined, temperature: 240 °C, pressure: 40 bar, H_2/CO: 2/1(mole ratio).

Results and Discussion

Catalyst Durability. In Fig. 2 are shown the changes in the rate of CO conversion, methane selectivity, and the rate of CO_2 formation for the synthesis gas reaction on a 2 wt% Ru/TiO_2 catalyst. It is clear that the catalytic activity (the rate of CO conversion) decreased constantly over 50 h of reaction. However, the methane selectivity was almost constant, irrespective of the catalytic activity. Although the reason of the decrease in the activity is not clear yet, it might be attributed to the coverage of ruthenium surface by carbon, as suggested by the marked decrease in the CO_2 formation, which should be attributed partly to the disproportionation of CO ($2CO \rightarrow C+CO_2$).

Effect of Carrier Materials. Tables 1 and 2 show the activities (formation rates of hydrocarbons and CO_2) and the selectivities (hydrocarbon distribution) of the slurry-phase F-T reaction using supported ruthenium catalysts which loaded 2 wt% ruthenium as metal. Most of the hydrocarbons were normal paraffins, and small amounts of isoparaffins and olefins were also produced. Formations of aldehydes and alcohols were quite small (less than 0.1% selectivity). The hydrocarbon distribution was well-simulated by the Anderson-Schulz-Flory (A-S-F) equation as demonstrated in Figs. 3 and 4. The plot is obviously divided into two straight lines. This fact has been observed also in the vapor-phase reaction, which has

Table 1. Activity and Selectivity of Supported Ruthenium Catalysts[a)]

Carrier	Dispersion	Formation rate		Product distribution/C-wt%					Chain-growth probability	
	%	H.C.[b)]	CO_2[c)]	C_1	C_2—C_4	C_5—C_{10}	C_{11}—C_{20}	C_{21}+	α_{15}+	α_{16}−
Aerosil SiO_2	26	626	0.92	8.8	8.6	27.0	30.0	25.7	0.89	0.93
TiO_2	88	350	3.06	9.1	17.1	30.3	26.5	17.0	0.86	0.92
Nb_2O_5	22	275	0.49	7.2	7.7	19.0	30.3	35.8	0.89	0.92
Aerosil-Al_2O_3	61	207	0.51	15.3	19.6	39.2	16.6	9.3	0.76	0.91
ZrO_2	10	172	0.42	8.5	9.5	21.6	36.1	24.3	0.92	0.92
γ-Al_2O_3-A	72	129	1.32	6.3	13.7	32.3	25.0	22.7	0.74	0.90
Ta_2O_5	10	86.8	0.29	12.5	12.4	21.0	21.7	32.5	0.85	0.93

a) 2 wt% loading of Ru; reaction temperature 240°C; total pressure 40 bar; $H_2/CO=2/1$ (mole ratio). b) mg-hydrocarbon $g^{-1}h^{-1}$. c) mmol-CO_2 $g^{-1}h^{-1}$.

Table 2. Activity and Selectivity of Alumina-Supported Ruthenium Catalysts[a)]

Carrier	Formation rate		Product distribution/C-wt%					Chain-growth probability	
	Hydrocarbon[b)]	CO_2[c)]	C_1	C_2—C_4	C_5—C_{10}	C_{11}—C_{20}	C_{21}+	α_{15}−	α_{16}+
γ-Al_2O_3-A	129	1.32	6.3	13.7	32.3	25.0	22.7	0.74	0.90
γ-Al_2O_3-B	23.5	0.21	31.9	31.9	22.3	10.3	3.6	0.55	0.88
γ-Al_2O_3-C	207	0.51	15.3	19.6	39.2	16.6	9.3	0.76	0.90
γ-Al_2O_3-D	190	0.55	10.8	14.6	35.3	23.9	15.4	0.82	0.91
γ-Al_2O_3-E	209	0.75	11.1	17.9	30.9	19.8	20.4	0.78	0.92
γ-Al_2O_3-F	232	0.99	12.5	17.1	35.0	21.0	14.4	0.77	0.90
α-Al_2O_3	16.8	0.05	21.7	25.7	28.3	16.5	7.8	0.78	0.88

a) 2 wt% loading of Ru; reaction temperature 240°C; total pressure 40 bar; $H_2/CO=2/1$ (mole ratio). b) mg-hydrocarbon $g^{-1}h^{-1}$. c) mmol-CO_2 $g^{-1}h^{-1}$.

been most likely attributed to the wide distribution of ruthenium particles.[7)]

As shown in Table 1 and Figs. 3 and 4, the activities and/or selectivities of the catalysts are markedly different from one another depending on the kind of the carrier materials even if they load the same amount of ruthenium. Especially, the ruthenium supported on TiO_2, Aerosil SiO_2 and Nb_2O_5 showed the high activities and the high chain-growth abilities when they

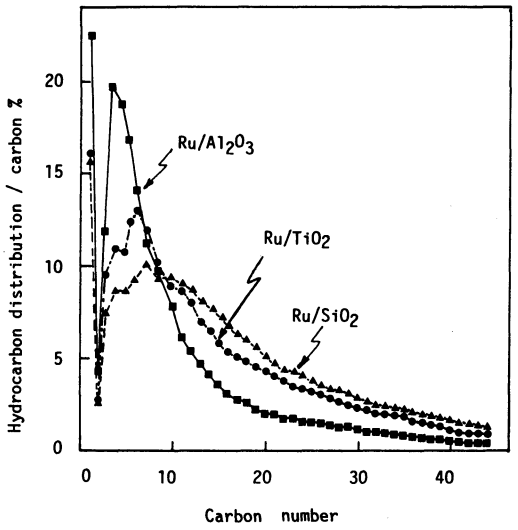

Fig. 3. Hydrocarbon distribution of the products on supported ruthenium catalyst. 2 wt% Ru on carriers, temperature: 240°C, pressure: 40 bar, H_2/CO: 2/1 (mole ratio).

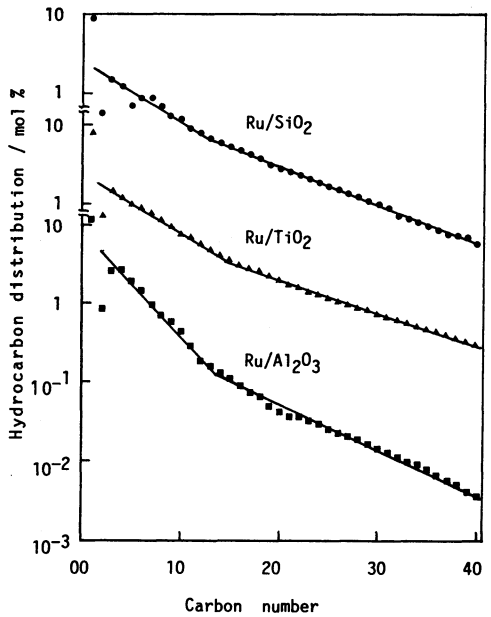

Fig. 4. Anderson-Schulz-Flory plot of the products. The same experiment as in Fig. 3.

were reduced without any pretreatment. This is the same trend which has been observed in the vapor-phase reaction over the same catalyst.[3)] It should be also noted that the Ru/TiO_2 catalyst made more CO_2 than other catalysts. The formation of CO_2 could be attributed mostly to the CO shift reaction of the product water. The high CO shift activity of the Ru/TiO_2 catalyst has been already reported by Kikuchi et al.[8)]

The high abilities of C-C chain growth of the Nb_2O_5-, ZrO_2-, and Ta_2O_5-supported catalysts have been observed also in the vapor-phase reaction.[7] As has been reported by us, the ruthenium particles with low dispersion are suitable for the production of high-molecular-weight hydrocarbons. The ruthenium dispersions on the carrier materials mentioned above are all lower than 20% (Table 1). Thus, their high chain-growth ability should be cased by the low dispersion of ruthenium particles.

The data in Table 2 shows that both the activity and selectivity vary with the kinds of the alumina carriers. Especially, the Ru/γ-Al_2O_3-B catalyst showed an extraordinary low activity and a low chain-growth ability. It could be attributed to sulfur-poisoning effect, because the carrier material which was prepared from aluminum sulfate contained SO_4^{2-} (about 2 wt%) and the sulfate ion is converted to hydrogen sulfide during the hydrogen treatment to poison the ruthenium. Although the reason why the chain-growth probability on the γ-Al_2O_3-B is lower than other alumina-supported ruthenium catalyst is not clear yet, the phenomenon itself is similar to that of a sulfur-poisoned cobalt catalyst,[9] Other γ-Al_2O_3-supported catalysts exhibited the similar activity and selectivity except the γ-Al_2O_3-based catalyst. Its reason will be discussed in the later chapter.

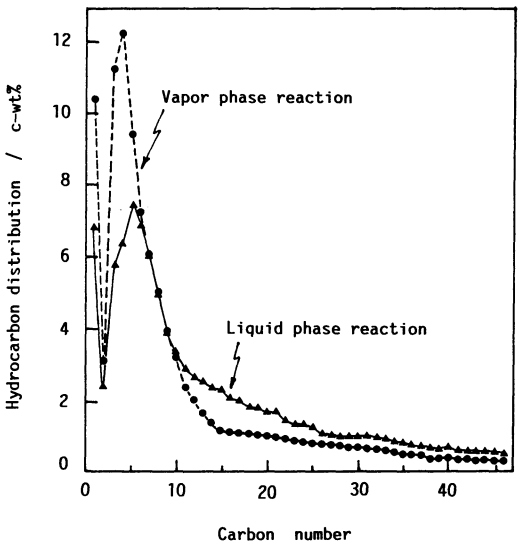

Fig. 5. Hydrocarbon distribution of the products from the vapor-phase reaction and the slurry-phase reaction. 2wt% Ru/TiO_2; noncalcined, temperature: 230°C (vapor phase); 240°C (slurry phase), pressure: 20 bar (vapor phase); 40 bar (slurry phase), H_2/CO: 2/1 (mole ratio).

In Fig. 5 are compared the difference in the hydrocarbon distribution between the products from the vapor-phase reaction and those from the liquid-phase reaction using the same catalyst. Obviously, the product from the vapor-phase reaction is rich in lower hydrocarbons. However, the degrees of chain-growth probability of both systems are very close, for example α_{15^-} and α_{16^+} are 0.72 and 0.88 for the vapor-phase reaction and 0.80 and 0.92 for the liquid-phase reaction. The higher selectivity of the high-molecular weight fraction in the liquid-phase reaction should be attributed to the fact that the higher fraction stays in the reactor and might grow further, whereas the lower fraction comes out of the reactor quickly.

Preparative Factors Which Control Catalytic Features. a. Metal Lording: As shown in Table 3, the rate of hydrocarbon formation increases with the increase in the metal loading on the catalyst weight base, while the dispersion of ruthenium decreases monotonously with increasing metal loading. It should be noted that the specific activity of ruthenium (the rate of hydrocarbon formation per unit weight of ruthenium) increases with increasing metal loading up to 2 wt%. It could be attributed to the decrease in the ruthenium dispersion. As previously reported by the present authors,[7] the catalytic activity of a low-dispersion-catalyst increases almost proportionally to the operating pressure up to 20 bar or higher in the vapor-phase reaction, while that of a high-dispersion catalyst levels off at 6 bar or lower. Thus, under the present reaction conditions where the operating pressure is 40 bar, the specific activity of the low-dispersion catalyst is higher than that of the high-dispersion catalyst.

Another charateristic feature wnich should be noted is that the chain-growth probility increased with the increase in the metal loading up to 2 wt% as shown in Table 3 and Fig. 6. This phenomenon is also attributable to their metal dispersions. It has been demon-

Table 3. Catalytic Features of Titania-Supported Ruthenium Catalysts[a)]

Loading	Dispersion	Rate of formation		TOF[d)]	Product distribution/C-wt%					Chain-growth probability	
wt%	%	H.C.[b)]	CO_2[c)]	$10^{-3}s^{-1}$	C_1	C_2—C_4	C_5—C_{10}	C_{11}—C_{20}	C_{21+}	α_{15^-}	α_{16^+}
0.2	87	9.8 (4.9)[e)]	2.0	13	20.5	23.9	24.7	21.1	9.7	0.62	0.87
0.5	88	16.2 (3.2)	0.9	8	19.9	31.1	31.4	12.5	5.1	0.70	0.86
1.0	83	70.9 (7.1)	2.9	20	17.8	28.6	29.2	19.1	4.8	0.64	0.85
2.0	55	318 (16.0)	3.1	67	9.1	9.1	26.5	29.0	26.3	0.85	0.92
4.0	46	480 (12.0)	1.6	63	9.9	13.9	29.4	22.4	24.4	0.83	0.93

a) Reaction temperature 240°C; total pressure 40 bar; $H_2/CO=2/1$ (mole ratio). b) mg-hydrocarbon $g^{-1}h^{-1}$. c) mmol-CO_2 $g^{-1}h^{-1}$. d) Turnover frequency. e) g-hydrocarbon (g-Ru)$^{-1}h^{-1}$.

strated by several research groups that the chain growth probability on supported ruthenium catalysts increases with the decrease in the ruthenium dispersion.[7,10,11] However, the change of metal loading is less effective in changing its activity and selectivity than the air calcination treatment, which has been pointed out in the vapor-phase reaction[7] and also will be discussed in the later chapter of this report. It could be explained in terms of two reasons. One is that the change in the dispersion level with the change in the loading is not so remarkable as that of air calcination. For example, the dispersion of a 4 wt% Ru/TiO_2, which has the lowest dispersion (46%), is about half of the dispersion of a 0.2 wt% Ru/TiO_2 (88%), which has the highest dispersion, whereas the dispersion level of a 2 wt% Ru/γ-alumina decreases from 72 to 12% with the rise in the calcination temperature from 120 to 400 °C. The present authors have pointed out that the turnover frequency (TOF) and the chain-growing ability of a supported ruthenium catalyst are markedly promoted when the average dispersion of ruthenium particles (measured by CO chemisorption) is less than about 20%.[7] Another is a more important reason that the particles of ruthenium metal formed by the conventional impregnation method have a wide distribution in size.[2] Thus, the unlcined catalyst should have much small particles as well as large particles as demonstrated by an A-S-F plot of the product with a winding point (Fig. 6). As the result, the characters of large particles should be diluted by those of small particles.

b. Air Calcination: It is possible to change the activity and selectivity of the supported catalysts by means of air calcination before hydrogen reduction.[3,4] In Table 4 and Fig. 7 are shown the dispersion, the catalytic activity, the TOF, and the product selectivity of the 2 wt% Ru/γ-Al_2O_3 catalysts which have been

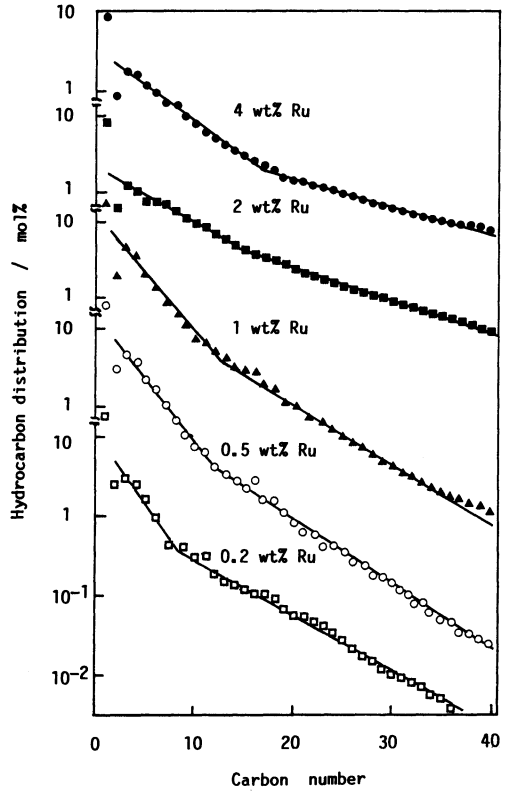

Fig. 6. Effect of metal loading on the hydrocarbon distribution of titania-supported ruthenium catalysts. The same reaction conditions as in Table 3.

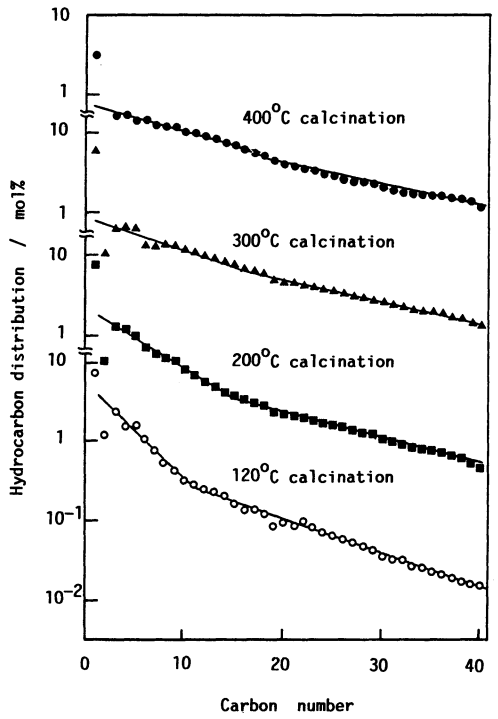

Fig. 7. Effect of calcination temperature on the hydrocarbon distribution of γ-alumina-supported ruthenium catalysts. 2 wt% Ru/γ-Al_2O_3-A, The same reaction conditions as in Table 4.

Table 4. Effect of Air Calcination on Physical and Catalytic Properties of γ-Alumina Supported Ruthenium Catalysts[a]

Calcination temperature	Rate of formation		Dispersion	TOF[d]	Product distribution/C-wt%					Chain-growth probability	
°C	H.C.[b]	CO_2[c]	%	$10^{-3}s^{-1}$	C_1	C_2—C_4	C_5—C_{10}	C_{11}—C_{20}	C_{21}+	α_{15}−	α_{16}+
120	129	1.32	72	25	6.3	13.7	32.3	25.0	22.3	0.74	0.91
200	227	1.75	78	40	7.6	9.8	23.9	26.2	32.6	0.86	0.93
300	250	0.77	36	98	5.9	5.0	17.1	30.0	42.0	0.91	0.94
400	218	0.37	12	246	3.2	4.1	17.6	31.6	43.5	0.93	0.94

a) 2 wt% loading of Ru; reaction temperature 240 °C; total pressure 40 bar; $H_2/CO=2/1$ (mole ratio). b) mg-hydrocarbon $g^{-1}h^{-1}$. c) mmol-CO_2 $g^{-1}h^{-1}$. d) Turnover frequency.

calcined in air at temperatures from 120 to 400 °C before reduction. The rate of hydrocarbon formation was promoted twice by calcining the virgin catalyst at 200 °C. Also the TOF was increased from 25×10^{-3} to $40\times10^{-3}\,s^{-1}$ by calcining at 200 °C. Above 200 °C, the rate of hydrocarbon formation per unit weight of ruthenium is almost constant irrespective of the calcination temperature up to 400 °C. However, the TOF increased from 40×10^{-3} to $246\times10^{-3}\,s^{-1}$ as the calcination temperature was increased from 200 to 400 °C. Concerning the product selectivity, the rate of CO_2 formation decreased and the chain growth-probability of the product was increased as the calcination temperature was increased. It should be attributed to the fact that the ruthenium dispersion decreased from 79 to 12% as the calcination temperature was increased from 200 to 400 °C. Also, it means that the surface character was changed as the ruthenium dispersion decreased.

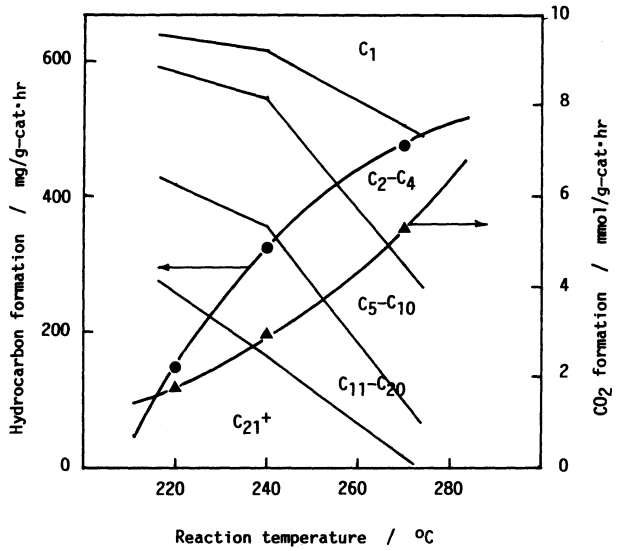

Fig. 8. Temperature effects on the slurry-phase Fischer-Tropsch synthesis on a 2wt% Ru/TiO_2 (non-calcined) catalyst. Pressure: 40 bar, H_2/CO: 2/1 (mole ratio).

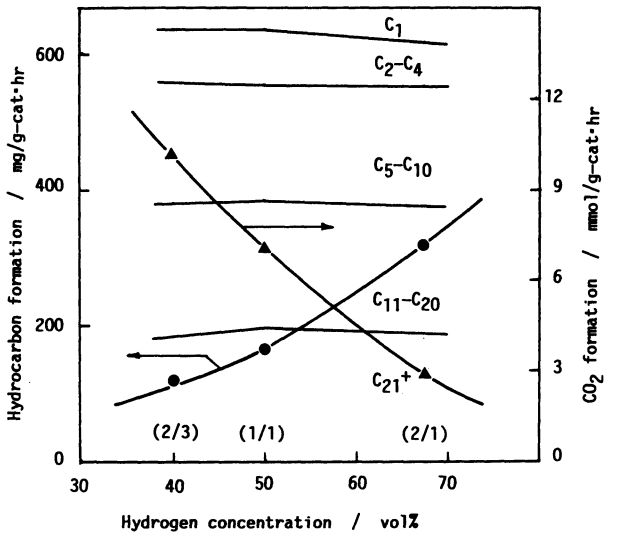

Fig. 9. Effects of feed gas composition on the slurry-phase Fischer-Tropsch synthesis on a 2wt% Ru/TiO_2 (noncalcined) catalyst. Temperature: 240 °C, pressure: 40 bar. Figures in parenthesis express the H_2/CO mole ratio in the feed gas.

Effect of Operating Factors on the Activity and Selectivity. Reaction Temperature: As is shown in Fig. 8, the rate of hydrocarbon formation on the Ru/TiO_2 catalyst was increased with increasing reaction temperature from 220 to 270 °C. The observed apparent activation energy for the hydrocarbon formation was about 12 kcal mol^{-1}. The rate of carbon dioxide formation was also increased with the rise of the reaction temperature, most likely due to the increase in the rate of water-gas shift reaction. In regard to the hydrocarbon distribution, the fraction of low-boiling hydrocarbons (C_1—C_4, especially methane) was increased drastically, which resulted in the change of the chain-growth probability (α) from 0.81 (220 °C) to 0.66 (270 °C).

H_2/CO Ratio of Feed Gas: Figure 9 also shows the effect of the H_2/CO ratio of the feed gas under the standard total pressure (40 bar). With the decrease in the H_2/CO ratio (2/1 to 2/3), the rates of hydrocarbon formation was decreased. These results are quite reasonable because the reaction rate on the ruthenium catalyst is usually first-order with respect to the partial pressure of hydrogen and zero or negative order with respect to the partial pressure of carbon monoxide[13] and because the solubility of either hydrogen or carbon monoxide in the solvent follows the Henry's law. As shown in Fig. 9, the hydrocarbon distribution obtained on a TiO_2-supported ruthenium catalyst was scarcely affected by the H_2/CO ratio. This result is in contrast to the characters on iron catalyst,[14] cobalt,[15] and ruthenium catalysts[16] in the vapor-phase reaction, which are markedly affected by the H_2/CO ratio. The fact that the hydrocarbon distribution is hardly affected by the H_2/CO ratio in the feed gas is one of the special features of the liquid-phase F-T synthesis with supported ruthenium catalysts, which should be studied further.

Conclusion

Highly active and selective ruthenium catalysts for Fischer-Tropsch synthesis were prepared by impregnating $RuCl_3$ on TiO_2, Nb_2O_5, or SiO_2 and then reducing in flowing hydrogen or by impregnating $RuCl_3$ on sulfur free γ-Al_2O_3, calcining at 300 °C or above, and then reducing. They were favorably used in the slurry-phase reaction.

The slurry-phase Fischer-Tropsch synthesis showed characters which was substantially similar to those of the vapor-phase reaction, but produced higher hydrocarbons with higher selectivity. However, no wax trouble was encountered under any conditions. The most effective condition could be chosen for the liquid

hydrocarbon synthesis. For instance, the highest selectivity of kerosene and gas oil (C_{11}—C_{20} hydrocarbons) calculated from the Anderson-Schulz-Flory distribution is 32.5% (α=0.87), while their highest selectivity value, 31.6%, was obtained in this study when the 2 wt% Ru/γ-Al_2O_3-A catalyst calcined in air at 400 °C was used with no troubles in spite of the high wax (C_{21}^+) selectivity, 43.5%.

Financial support by the Grant-in-Aid for Energy Research from the Ministry of Education, Science and Culture is greatly acknowledged.

References

1) H. Koelbel, P. Ackerman, and F. Engerhardt, *Erdoel Kohle*, **9**, 153, 225, 303 (1956).
2) H. Koelbel and M. Ralek, *Catal. Rev. Sci. Eng.*, **21**, 225 (1980).
3) M. L. Riekena, A. G. Vickers, E. C. Haun, and R. C. Koltz, *Chem. Eng. Prog.*, April 86 (1982).
4) C. C. Hall and D. Gall, *J. Inst. Petrol.*, **38**, 845 (1952).
5) T. Kunugi, T. Sakai, and N. Negishi, *J. Jpn. Petrol. Inst.*, **11**, 636 (1968).
6) M. Sclesinger, M. Crowel, and M. Leva, *Ind. Eng. Chem.*, **43**, 1474 (1951).
7) K. Fujimoto, T. Nobusawa, T. Fukushima and H. Tominaga, *Bull. Chem. Soc. Japan.*, **58**, 3164 (1985).
8) E. Kikuchi, H. Nomura, M. Matsumoto, and Y. Morita, *App. Catal.*, **7**, 1 (1983).
9) R. J. Madon and H. Shaw, *Catal. Rev.-Sci. Eng.*, **15**, 69 (1977).
10) C. S. Kellner and A. T. Bell, *J. Catal.*, **71**, 288 (1981).
11) R. C. Everson, K. J. Smith, and E. T. Woodburn, *Proc. Int. Mtg. S. Afr. Inst. Chem. Eng.*, (1980).
12) J. R. Anderson, "Structure of Metallic Catalysts," Academic Press (1975).
13) M. A. Vannice, *Catal. Rev. Sci. Eng.*, **14**, 153 (1976).
14) M. E. Dry, *Catalysis*, **1**, 159 (1981).
15) K. Fujimoto, H. Saima, and H. Tominaga, *J. Jpn. Petrol. Inst.*, **26**, 258 (1983).
16) F. S. Karn, J. F. Shultz, and R. B. Anderson, *Ind. Eng. Chem., Prod. Res. Dev.*, **4**, 265 (1965).